frontiers | Frontiers in Materials

TYPE Original Research
PUBLISHED 29 September 2025
DOI 10.3389/fmats.2025.1603074

Check for updates

OPEN ACCESS

EDITED BY
Olivia Martius,
University of Bern, Switzerland

REVIEWED BY
Mohammad M. Karimi,
Tarbiat Modares University, Iran
Timo Schmid,
ETH Zürich, Switzerland

*CORRESPONDENCE
Brenna Meisenzahl,
bmeisenzahl@ibhs.org

RECEIVED 08 April 2025
ACCEPTED 10 September 2025
PUBLISHED 29 September 2025

CITATION
Meisenzahl B, Giammanco I and Hedayati F (2025) Sub-severe hail: the missing piece in assessing asphalt shingle risk in North America.
Front. Mater. 12:1603074.
doi: 10.3389/fmats.2025.1603074

COPYRIGHT
© 2025 Meisenzahl, Giammanco and Hedayati. This is an open-access article distributed under the terms of the Creative Commons Attribution License (CC BY). The use, distribution or reproduction in other forums is permitted, provided the original author(s) and the copyright owner(s) are credited and that the original publication in this journal is cited, in accordance with accepted academic practice. No use, distribution or reproduction is permitted which does not comply with these terms.

Sub-severe hail: the missing piece in assessing asphalt shingle risk in North America

Brenna Meisenzahl*, Ian Giammanco and Faraz Hedayati

The Insurance Institute for Business and Home Safety, Richburg, SC, United States

Hail risk is a growing problem for homeowners and insurers, particularly as insurance claims analysis reveal that asphalt shingle roofs are sustaining damage from hailstone sizes previously thought not to affect most roofing materials. Research by the Insurance Institute for Business and Home Safety indicates that sub-severe hail falls more frequently than large hail, leading the authors to believe that the cumulative damage from repeated sub-severe exposure is much higher than previously expected. To investigate this hypothesis, observations of these types of hail events were applied to conduct laboratory testing of asphalt shingles. A high concentration, sub-severe hail event was recreated in a controlled laboratory setting and used multiple times to test both experimental and control asphalt shingle test specimens, followed by exposure to a large hail event. The experimental group was exposed to natural weathering between sub-severe hail exposures to reflect real-world aging conditions. Both groups were compared to the new product performance against only large hail impacts (baseline)—image processing techniques allowed for the evaluation of damage and quantitative granule loss measurements. The results showed that exposure to high concentrations of small hailstones can significantly reduce the roof cover's resistance to future large hail events and exacerbate the natural aging of asphalt shingles. This suggests that frequent sub-severe hailstorms may pose a greater threat to roof longevity than previously recognized and is a driving factor in the growing hail risk in the United States that is not accounted for in current durability standards or risk assessments.

KEYWORDS

asphalt shingle roofs, sub-severe hail, large hail, asphalt shingles, granule loss, natural weathering, hailstorms

1 Introduction

Increased awareness of hail-related risks has highlighted the need for inclusive hail size data within the insurance industry. In their 2022 financial reports, three of the five largest publicly traded Property and Casualty (P&C) insurers identified hail as a significant issue (ZestyAI, 2023). Asphalt shingles comprise approximately 80% of roof coverings for residential homes in the United States (Freedonia Group, 2024). In 2023, global insured losses from severe convective storms (SCS) reached a record high of $64 billion, with the United States accounting for 85% of those losses (Swiss Re Institute, 2024). According to Aon, the United States reported over $50 billion in SCS-related insured losses in 2023 and is projected to surpass that record in 2024 (Evan, 2024). Hail has moved to the forefront of loss drivers and will continue to impact home and

business owners, as it is responsible for an estimated 50%–80% of annual damages SCS events (CAPE Analytics, 2025).

The National Weather Service (NWS) classifies hail as severe when its diameter exceeds 25.4 mm, and anything between 5 mm (graupel) and 25.4 mm is considered sub-severe. According to a 2022 study (Elmore et al., 2022), each year, several hail-day maxima are primarily influenced by sub-severe hail rather than severe hail. The highest occurrence frequency is observed in Oklahoma, with approximately 28 days of activity per year (the peak severe hail is a 20-day maximum across the tristate area of Nebraska, Kansas, and Colorado) (Elmore et al., 2022). There is a clearer understanding of the impacts large hail has on asphalt shingle roofs, given that large or severe hail has been the predominant focus of prior hail studies. The resistance of asphalt shingle roofing products to hail varies depending on the material properties of both the shingles and the hailstones (Brown-Giammanco et al., 2021). Research conducted at the Insurance Institute for Business and Home Safety (hereinafter referred to as IBHS) has provided insight into the various damage modes caused by large hail on asphalt shingles. However, sub-severe hail is poorly understood, with an unknown damage potential (Elmore et al., 2022), as their effects have yet to be studied in detail. Though smaller stones individually cause less damage, sub-severe hailstones are far more common than the rare large hailstones and result in the vast majority of granule loss. Granules serve more than an aesthetic purpose on asphalt shingles; their primary role is to protect the underlying asphalt. Once those granules are displaced, the asphalt is exposed to UV radiation and becomes more brittle, exacerbating the natural aging process.

Understanding the effects of small hailstones impacting asphalt shingles is critical to understanding the increasing damage from hailstorms across North America, particularly in the United States, as these roof cover types are highly susceptible to hail damage. Residents in hail-prone regions, such as the Dallas-Fort Worth (DFW) area, may need to replace their roofs multiple times within 10 years (Brown et al., 2015). Because sub-severe hail falls below the conventional threshold for severe classification, Marshall (1999) suggests that hailstones smaller than 25.4 mm (1 inch) rarely cause functional damage. Functional (claim-worthy) damage from hail is defined as punctures or fractures in the shingle that compromise its water-shedding capability or reduce its service life (Smith, 2013). We hypothesize that repeated exposure to these sub-severe events may dislodge enough granules to accelerate shingle deterioration, increasing vulnerability to future hail damage. To simulate this effect, our testing incorporated a high concentration hail scenario, characterized by a dense accumulation of hail over a small area within a relatively short timeframe. While there is no standardized threshold for what constitutes "high concentration" hail, we selected 44 impacts per square foot (0.09 per m^2), based on available field data, to represent a realistic estimate of sub-severe hail exposure. It is crucial to understand the climatology of all types of hail, as even sub-severe hail can cause substantial roof damage over time with repeated exposure. The experimental goals of this study were as follows:

- Evaluate if high concentrations of sub-severe hailstones result in sensible damage to asphalt shingle products.
- Quantify the relationship between standard granular adhesion test methods and laboratory hail impact performance.
- Evaluate if asphalt shingles exposed to a high concentration of sub-severe hail will exhibit degraded performance after 2 years of natural weathering compared to a control group that was not weathered.
- Compare laboratory test results to previous large hail analysis to determine if areas that experience these events more frequently are more prone to roof cover damage.

2 Materials and methods

2.1 Approach and procedure

In this study, we employed machine vision techniques to assess and quantify granule loss damage resulting from sub-severe impacts observed on a subset of common asphalt shingle products. Testing consisted of simulating exposure to two high concentration sub-severe hail events in the laboratory using ice spheres of 17.8 mm (0.7 in.) and 25.4 mm (1 in.) in size and focusing on the cumulative effects of sub-severe hail as opposed to individual impacts, which is the focus of typical standardized testing for asphalt shingles. Natural weathering was integrated between test series to understand the effects of these types of events over time. Finally, products were also subjected to the impacts of large hailstones and their damage compared to previous research on the performance of brand-new products to large hail with no prior sub-severe exposure. The experimental procedure included 1 year of natural weathering prior to hail impact testing, along with photographic documentation of each test specimen before and after impact testing for analysis. These steps were performed a second time prior to large hail impacts. Details are outlined in Table 1.

2.2 Test specimens

To accomplish the objectives, six asphalt shingle products from different manufacturers were selected for this study. These products included four impact-resistant (IR) and two conventional oxidized shingles, with both three-tab and architectural designs (Figure 1).

Two 1.3-m by 17-m (50 in. by 66 in.) test specimens were constructed of each product, following the ASTM D3161 wind test requirements, with shingles installed according to their manufacturers' instructions (ASTM, 2020). One test specimen of each product was placed in the experimental group to undergo natural weathering. In contrast, the second test specimen of each product was placed in the control group and stored in a climate-controlled interior storage space for a period of 1 year. A third group was considered the baseline, and these test specimens were not subjected to natural weathering or sub-severe hail and were only impacted by a set number of larger hailstones. A rack system was constructed on the IBHS Aging Farm in Richburg, South Carolina, for the experimental group of test specimens to be placed facing south and exposed to natural weathering for 1 year at a time (Figure 1). During this time, the controlled group remained in a conditioned storage space untouched (Figure 1).

TABLE 1 Experimental procedures and timeline.

Step	Procedure
1	One year: Natural weathering (experimental group) and conditioned storage (control group)
2	Pre-impact photographic documentation of all test specimens
3	Test series 1: Impact testing of ice spheres to replicate sub-severe hail on all test specimens
4	Post-impact photographic documentation and test series 1 image analysis
5	One year: Natural weathering (experimental group) and conditioned storage (control group)
6	Pre-impact photographic documentation of all test specimens
7	Test series 2: Impact testing of ice spheres to replicate sub-severe hail on all test specimens
8	Post-impact photographic documentation and test series 2 image analysis
9	Test series 3: Impact testing of large hail on all test specimens
10	Post-impact photographic documentation and test series 3 image analysis
11	Full damage evaluation
12	Statistical analysis and results compilation

2.3 Image apparatus

While some granule loss on asphalt shingles can be observed with the naked eye, visually quantifying the extent of damage is often impractical for this type of damage mode. To overcome this limitation, a machine vision algorithm was developed to assess granule loss across an entire test specimen precisely. To accurately assess each test specimen, high-quality photographs of the test specimen were captured prior to hailstone impacts, using a custom-designed camera rig featuring controlled lighting, camera mounts, and the ability to remove shadowing (Figure 2). The rig was constructed out of 80/20 aluminum, featuring a modular framing system allowing for easy assembly with connectors and fasteners. The rig dimensions are 1.9 m by 1.3 m by 1.8 m (75 in. by 51 in. by 70 in.) with the test specimen in place. Four LED lights were placed 3 ft above the test specimen, within fitted spaces of the 80/20 to ensure image consistency for photographic documentation. Dark blackout curtains were hung along each side of the rig to eliminate any outside shadows and provide optimal image quality, as shown in Figure 2. Next to each LED light was a 3D-printed camera mold to hold a Sony RX100 camera. High-resolution camera settings were necessary for image quality and processing. A Bluetooth remote control allowed the camera to be controlled from the ground. These factors were carefully fine-tuned to ensure consistent imaging across all test specimens, minimizing any potential variability in the photographic process. The height of the camera placement was determined based on the image quality of individual granules, although this does not allow for viewing the entire specimen in a single image. To solve this issue, each test specimen was divided into four quadrants using a chalk line, and photographic documentation of each quadrant was captured.

2.4 Hailstones and impact testing

2.4.1 Sub-severe hail

For the sub-severe experiments, ice spheres were produced in molds using tap water (Figure 3). Molds were used for this ice since the IBHS laboratory hail manufacturing system—a machine typically used to create scientific laboratory hailstones—was unable to produce the small sizes necessary for this testing. The two molds used consisted of 25.4 mm (1 in.) diameter spheres (Figure 3b) and 17.8 mm (0.7 in.) diameter spheres (Figure 3b). Once filled with water, the molds were clamped down using quick-grip clamps and then placed in a freezer. After at least 24 h in the freezer, the ice spheres are removed from the molds, shaving off any protrusions, and placed in flat egg cartons. They are then stored in a freezer, ready to be used for impact testing. Each ice sphere's weight and diameter are measured and recorded prior to the ice sphere being loaded in a hail cannon for impact testing. The hail cannon apparatus utilizes compressed air, an accumulator tank, a large quick-opening valve, and interchangeable barrels to accommodate various hailstone sizes, enabling propulsion of the ice spheres at roofing products at speeds that mimic the velocity of hail (Figure 4a). The hail cannon was calibrated prior to testing as part of quality control measures. Both radar and chronograph devices were used to read the speed of projected ice spheres (Figure 4c). The target kinetic energy for ice spheres used in this testing was calculated based on the mean diameter-to-kinetic energy relationship presented in Heymsfield et al. (2014), which is also incorporated in the IBHS Impact Resistance Test Protocol (Insurance Institute for Business and Home Safety, 2019). Although a revised relationship was later proposed by Heymsfield et al. (2018), the 2014 formulation was used to maintain consistency with the IBHS Impact Resistance Test Protocol applied in this experiment. The diameter-to-kinetic energy relationship equation used in this study is as follows:

$$\text{Mean, at 1000hPa: } KE = 0.0217 D_{max}^{4.31}$$

Each specimen was securely mounted on a base perpendicular to the trajectory of the hail cannon (Figure 4b). Test specimens were subjected to a simulated 500 hailstone impacts in a single test series: 300 ice spheres with a diameter of 17.8 mm (0.7 in.) and 200 ice spheres with a diameter of 25.4 mm (1 in.). The same test series was run twice for this experiment, resulting in a total of 1,000 ice spheres per test specimen. As mentioned in Table 1, the experimental group underwent 1 year of natural weathering at the beginning of test series 2 to mimic the natural exposure of a roof between hailstorms. Natural weathering processes, such as ultraviolet (UV) radiation, thermal cycling, and moisture exposure, are known to affect a roof's vulnerability to impact damage over time. To enhance the realism of the experiment, impact locations were neither predetermined nor marked, ensuring a random distribution of impacts across the test specimens and allowing the possibility that the exact location could be struck multiple times. Each ice sphere must meet the specified

10.3389/fmats.2025.1603074

FIGURE 1
Test specimen setup for the experimental and control groups, including two experimental test specimens on outdoor racks to be naturally weathered for a period of 1 year (the process was repeated). Experimental test specimen **(a)** shows a 3-tab asphalt shingle product compared to experimental test specimen **(b)**, with an architectural shingle. All control test specimens **(c)** are in a climate-controlled storage space between impact test series. **(a)** A 3-tab conventional asphalt shingle test specimen from the experimental group. **(b)** An impact-resistant architectural shingle test specimen from the experimental group. **(c)** Control test specimens stored on a rack, protecting the surface of the asphalt shingles, in a climate-controlled space.

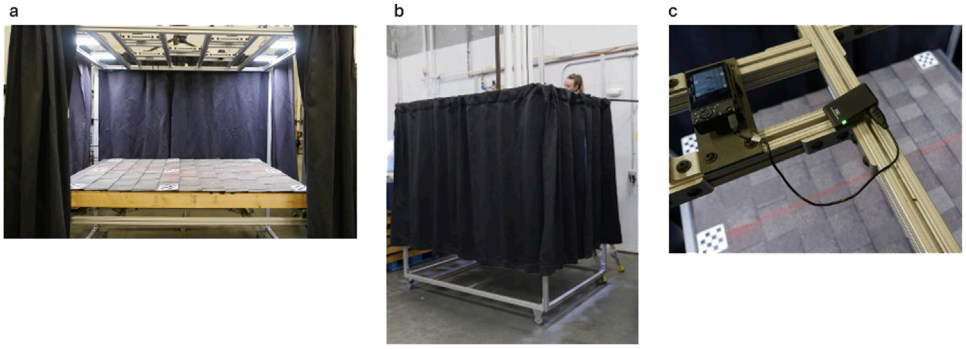

FIGURE 2
Custom camera rig designed to capture images of asphalt shingle test specimens. The rig, designed out of 80/20, featured controlled lighting, fixed camera mounts, and features designed to minimize shadowing, ensuring high image quality for accurate assessments. **(a)** Interior view of the imaging area with a mounted asphalt shingle specimen and controlled lighting. **(b)** Exterior view of the custom rig with curtains to minimize shadowing **(c)** Overhead view of the mounted camera design aligned with a quadrant of the test specimen.

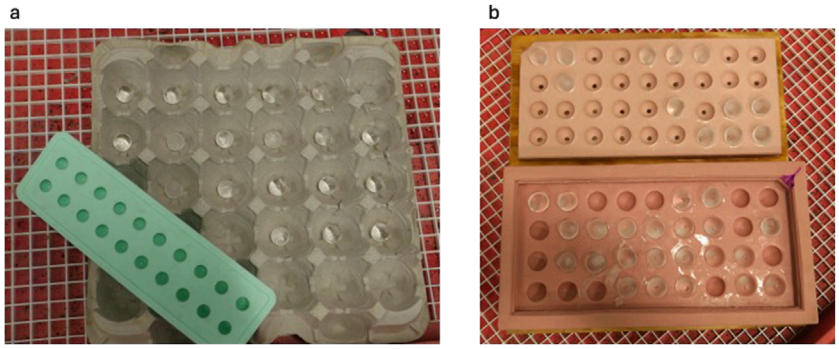

FIGURE 3
Molds used to make 17.8 mm (0.7-inch) and 25.4 mm (1-inch) ice spheres. After freezing for at least 24 h, the ice spheres are removed from the molds and any major imperfections (such as an ice stem on the 25.4 mm spheres) were cut off. Ice spheres were placed in egg cartons, as seen in **(a)**, and placed back into the freezer to be used for impacting. Molds are consistently refilled once empty to maintain ice sphere supply. **(a)** 17.8 mm (1 in.) ice mold and egg carton. **(b)** 25.4 mm (1 in.) ice mold.

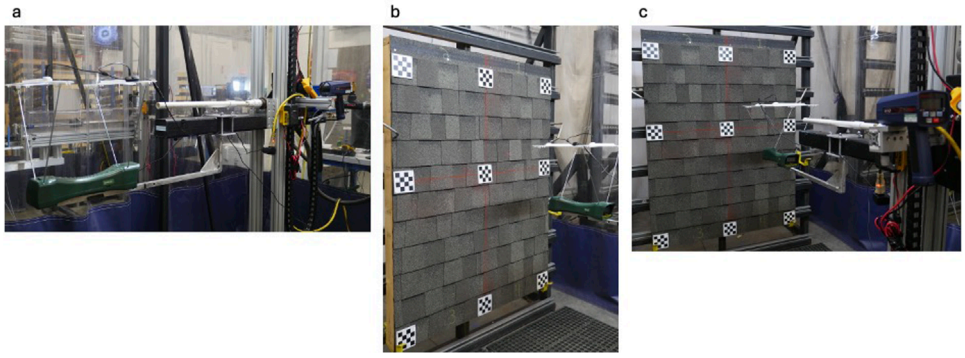

FIGURE 4
Hail cannon apparatus used to impact asphalt shingles test specimens with ice spheres and lab-manufactured hailstones of various sizes using interchangeable barrels. **(a)** 17.8 mm (0.7 in.) barrel attached to a hail cannon, along with the radar and chronograph, placed in fixed locations to capture ice sphere speed. **(b)** Test Specimen mounted for impact testing **(c)** A hail cannon is set up in front of the test specimen.

TABLE 2 Specified ice sphere characteristics and acceptable variability ranges for impact testing of asphalt shingle products. Class represents the sub-severe ice sphere sizes used in this study: 1.7 cm (0.7 in.) and 2.54 cm (1 in.).

Class (cm)	Diameter (cm)	Mass (g)	Target kinetic energy range(J)
1.7	1.7±2%	2.45±20%	0.21–0.40
2.54	2.54±2%	8.45±20%	0.61–2.26

requirements as seen in Table 2. While transparent ice spheres must follow the specified mass and diameter criteria defined for sub-severe hail (Table 2), greater flexibility was allowed in stone selection for the sub-severe impacts than is allowed for lab-manufactured hail, which are more commonly used for testing building materials at IBHS. Clear ice can be challenging for radar-based speed detection or conventional chronographs to detect, particularly at the small projectile sizes used in this study. In instances where the velocity was not accurately detected or missed entirely, the speed of the previous hailstone was used to calculate the kinetic energy for that shot. Within test series 1, 97.3% of 17.8-mm (0.7-inch) and 98.6% of 25.4 mm (1 in.) ice sphere impacts were within acceptable kinetic energy ranges. These missed detections occurred infrequently and comprised a small fraction of the total shots. As such, this limitation was not expected to have significantly influenced the consistency of the test results or damage assessments. The focus of this study was on randomness and the cumulative effects of hailstones rather than on each impact or impact mode, making the precision of individual impacts of lesser importance. Once an ice sphere impacts the test specimen, it was counted toward the total required impacts for its respective size.

2.4.2 Large hail impacts

Test series 3 impacts followed the requirements and procedure for 50.8 mm (2 in.) hailstone impacts in the IBHS Impact Resistance Test Protocol for Asphalt Shingles (Insurance Institute for Business and Home Safety, 2019). This protocol evaluates the hail impact resistance of asphalt shingles using laboratory-manufactured hailstones that replicate the velocity and kinetic energy of natural hail. Damage is assessed across three categories—breach, deformation, and granule loss—to calculate a quantitative performance rating. In this context, "performance" refers to the relative ability of asphalt shingles to withstand hail impacts, as defined by Brown-Giammanco et al. (2021). As performance declines, shingles may no longer effectively fulfill their intended purpose. Unlike the sub-severe ice spheres used in this study, the 50.8 mm (2in.) laboratory-manufactured hailstones were produced by the IBHS laboratory hail manufacturing system, a specialized tool for creating simulated hailstones. Details regarding hailstone fabrication are provided in Brown-Giammanco et al. (2021).

Large hail impacts were subjected to single locations outlined prior to testing as described in the IBHS Impact Resistance Test Protocol for Asphalt Shingles (Brown-Giammanco et al., 2021). All large hail impacts were positioned at least 76.2 mm (3 in.) away from other impact locations across the test specimens, the outer edge of the test specimen, and the midspan support brace. For 3-tab shingle products, impacts were placed no closer than 25.4 mm (1 in.) from the edge of the shingle tab. For architectural products, impacts were required to both single- and multi-ply sections, ensuring a minimum distance of 25.4 mm (1 in.) from the shingle edge and from the transition between single- and multi-ply layers. For each specimen tested, 3-tab shingles were subjected to a total of 20 impacts across the field of the test specimen, consisting of ten hard mode impacts–including at least four hard shatter and four hard bounce impacts–as well as ten soft mode impacts to capture all known hail impact modes. Similarly, architectural shingles received a total of 40 impacts per specimen, with ten hard mode impacts distributed across both single- and multi-ply portions—ensuring at least four hard shatter and four hard bounce impacts on each–along with ten soft mode impacts on each portion. In cases where unintended

impact nodes occurred while attempting to achieve specific impact conditions, those impacts were discarded.

2.5 Damage evaluation using machine vision

2.5.1 Image processing for sub-severe impacts

In this study, damage identification of granule loss was conducted using image processing techniques. This approach involved comparing images taken before and after the impact on the shingles to detect and analyze areas of granule loss. Quantitative data were then assessed to determine the extent of the damage using pixel aspect ratio (PAR), providing a detailed evaluation of granule displacement and material degradation. Each quadrant of a test specimen was assessed individually before combining data from all four quadrants to determine the total granule loss. Pre- and post-impact images were first registered using Binary Robust Invariant Scalable Keypoints (BRISK). To enhance the quality of BRISK, checkerboard stickers were attached to the corners of each quadrant, enabling the algorithm to overlay images accurately. Once the post-impact photo was registered with the pre-impact photo, the former was subtracted from the latter to highlight the changes associated with granule loss. Using the known dimensions of the checkerboards, the pixel aspect ratio (PAR) was calculated to estimate the damage area from the binarized subtracted image accurately.

The algorithm was applied to each quadrant separately, and the results were combined, ensuring a comprehensive assessment of the shingle surface. A limitation exists where manual manipulation must be used during the process to select the color threshold. This manual manipulation can introduce a bias caused by the operator. The bias of a human user was mitigated by observing the impacted test specimen while running the photographic documentation through the image processing algorithm described. Observing the test specimen allows for the greatest accuracy in depicting granule loss in the algorithm to match the physical test specimen.

2.5.2 Hail impact parameterization system

In furthering the damage analysis, we used the IBHS-Nemesis Impact Damage Evaluation Tool, as described in (Brown-Giammanco et al., 2021), to collect data on deformation and breaches caused by the large hailstone impacts. Deformation refers to dents and ridges that are made in the shingles, quantified by volume. Breaches are 1-dimensional damage resulting in a tear or crack in the shingles, quantified by expert judgement. The damage evaluation tool is an image-processing-based application meant to analyze high-resolution photographs of tested shingle samples to quantify surface deformations. Multiple images were captured from various angles of each shingle with a 2-in hailstone impact. The images were processed to generate a three-dimensional representation of each impact site. The system applied custom algorithms to assess damage severity and measure the extent of material loss. The severity level and scoring for each damage mode were given based on the outlined criteria in the IBHS Impact Resistance Test Protocol for Asphalt Shingles. The severity level was set on a scale of 0–3 (least damage to most damage). Overall scores are assigned to each product on a scale of 0–3, based on numerically averaging the individual damage scores (Brown-Giammanco et al., 2021). A performance evaluation rating was then assigned to each asphalt shingle product/test specimen as either poor (>1.8), marginal (>1.2–1.8), good (>0.3–1.2), or excellent (0–0.3) performance. Performance ratings are compared to previously tested asphalt shingle products in both new and naturally weathered states. Similar to the image processing algorithm, a limitation exists due to possible human bias as a result of manual manipulation of granule loss thresholds. This limitation was mitigated by physically observing each impact being assessed, allowing for the closest depiction of granule loss for each 50.8 mm (2 in.) impact location.

3 Results

This section presents the granule loss observed after each test series of sub-severe impacts and its effect on subsequent damage from larger hail. Baseline data are compared with both experimental and control groups to evaluate the extent of damage. The results were analyzed following the procedures outlined in the IBHS Impact Resistance Test Protocol for Asphalt Shingles, and the performance of the tested products was compared to those same products having no prior aging or sub-severe impacts.

3.1 Simulated high concentration of sub-severe impact tests followed by large hail impacts on naturally weathered shingles

Each test specimen was subjected to an approximate total of 400 ice spheres of 25.4 mm (1 in.) diameter and 600 ice spheres of 17.8 mm (0.7 in.) diameter in random locations. Table 3 shows the amount of granule loss across each test specimen from sub-severe impacts after test series 1. Compared to the granule loss from a single 50.8-mm (2 in.) hailstone impact, the exact product would have experienced a similar amount of damage. The baseline test specimens were evaluated using both patch and individual granule loss, in accordance with the IBHS Impact Resistance Test Protocol (Insurance Institute for Business and Home Safety, 2019). Notably, the cumulative granule loss from the sub-severe impacts in test series 1 exceeded the total granule loss recorded under a single 50.8-mm hailstone impact, even when both patch and individual loss were considered.

Similarly, Table 4 shows the cumulative granule loss of test series 1 and 2. The data indicated that the naturally weathered experimental test specimen group experienced greater granule loss than the control group, which was only subjected to laboratory-conditioned space. Although it might be expected that impact-resistant shingles would outperform conventional shingles, Table 3 shows this was not consistently the case. For example, product 5 (P5), a conventional shingle, exhibited the worst granule loss among the control group specimens. In contrast, product 1(P1), a 3-tab impact-resistant shingle, showed the highest granule loss after 1 year of natural weathering. A few test specimens in the experimental group (naturally weathered) exhibited visibly noticeable granule

TABLE 3 Granule loss results and comparisons across all products from Test Series 1, compared to average granule loss from a single 2-inch (50.8 mm) hailstone impact. Pre-impact images for the P4 control product were unusable for the analysis, indicated by "N/A". The type of shingle is indicated as IR or Conv., distinguishing an impact resistant or conventional shingle.

Product ID	Type	Cumulative area of granule loss for control group specimens in mm^2 (in^2)	Cumulative area of granule loss for experimental group specimens in mm^2 (in^2)	Single 50.8 mm (2-inch) impact in the IBHS impact resistance test protocol for asphalt shingles (baseline)	
				Average individual granule loss in mm^2 (in^2)	Average patch granule loss in mm^2 (in^2)
P1	IR	5,871 (9.1)	7,032 (10.9)	Not tested, no longer available for purchase	
P2	Conv	5,612 (8.7)	6,322 (9.8)	19 (0.03)	10 (0.02)
P3	IR	2,967 (4.6)	4,838 (7.5)	18 (0.03)	28 (0.04)
P4	IR	N/A	3,290 (5.1)	7 (0.01)	4 (0.01)
P5	Conv	2,451 (3.8)	4,516 (7.0)	17 (0.03)	15 (0.02)
P6	IR	6,967 (10.8)	4,709 (7.3)	9 (0.01)	2 (0.01)

TABLE 4 Combined cumulative granule loss results from Test Series 1 and 2, compared to the average granule loss from a single large hail impact for each asphalt shingle product. The type of shingle is indicated as IR or Conv., distinguishing an impact resistant or conventional shingle.

Product ID	Type	Cumulative area of granule loss for control group specimens in mm^2 (in^2)	Cumulative area of granule loss for experimental group specimens in mm^2 (in^2)	Single 50.8 mm (2-inch) impact in the IBHS impact resistance test protocol for asphalt shingles (baseline)	
				Average individual granule loss in mm^2 (in^2)	Average patch granule loss in mm^2 (in^2)
P1	IR	9,716 (15.1)	11,531 (17.9)	Not tested, no longer available for purchase	
P2	Conv	9,166 (14.2)	11,882 (18.4)	19 (0.03)	10 (0.02)
P3	IR	5,742 (8.9)	8,450 (13.1)	18 (0.03)	28 (0.04)
P4	IR	2,528 (3.9)	6,138 (9.5)	7 (0.01)	4 (0.01)
P5	Conv	4,715 (7.3)	7,852 (12.2)	17 (0.03)	15 (0.02)
P6	IR	9,136 (14.2)	8,767 (13.6)	9 (0.01)	2 (0.01)

loss after testing. Among the impact-resistant shingles, performance varied, with some products (e.g., P4) maintaining relatively low granule loss even after natural weathering, while others (e.g., P1) exhibited a more pronounced decline in durability. No dents or tears were observed visually or detected from the high concentration of sub-severe impacts. Within the control group, a test specimen of product 4 (P4) was missing data points in the first test series of sub-severe impacts due to a picture quality issue that prevented us from processing the images correctly for the machine vision analysis. Missing a single data point resulted in a minor deviation from the granule loss average and totals for the control group. However, the overall results would not have diverged significantly with the inclusion of the product 4 (P4) control group test specimen data points.

Figure 5 additionally shows the granule loss from test series 3, consisting of 50.8 mm (2 in.) hailstone impacts. The number of larger hailstone impacts depends on whether the product was a 3-tab (20 impacts) or architectural (40 impacts) shingle, as previously discussed. All but one experimental (naturally weathered) test specimen showed much higher levels of granule loss in this testing series. Sub-severe impacts to the experimental test specimens caused an average of 5,117.8 mm^2 of granule loss in test series 1 and an additional 3,985.5 mm^2 of granule loss in test series 2. The control group observed an average of 4,773.6 mm^2 of granule loss in test series 1 and an additional 2,855.8 mm^2 of granule loss in test series 2. The importance of sub-severe impacts and natural weathering is shown in Figure 5, where naturally weathered product 6 (P6) experienced the highest total granule loss from test series 3 (50.8-mm hail impacts). Compared to product 6 (P6) in the control group, which experienced the lowest amount of granule loss in test series 3, it performed well in its non-weathered state. In test series 1, the experimental group exhibited a mean

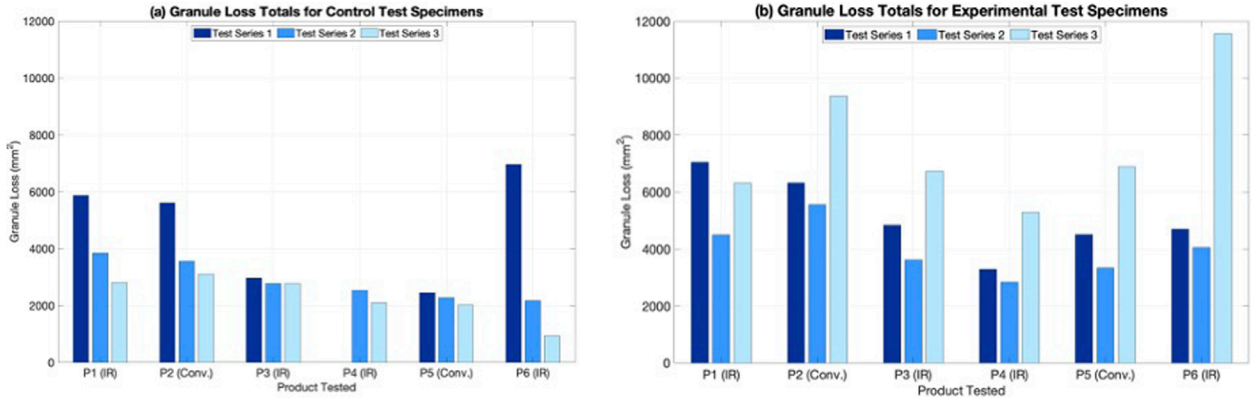

FIGURE 5
The total granule loss from each round of ice sphere and hail impacts is shown across all tested asphalt shingles products. Average granule loss from those test specimens in the control group **(a)** for each round was 4,773.6 mm^2, 2,855.8 mm^2, and 2,287.2 mm^2, respectively. Average granule loss from the experimental group (naturally weathered) test specimens **(b)** for each round was 5,117.8 mm^2, 3,985.5 mm^2, and 7,687.2 mm^2, respectively.

TABLE 5 Summarization of statistics of the granule loss data for experimental and control groups.

Shingle type	Group	Mean granule loss (mm^2)	Standard deviation (mm^2)	Standard error (mm^2)
Impact Resistant	Control	8,930.5	3,309.86	1,654.93
Conventional	Control	9,502.0	3,915.96	2,769.00
Impact Resistant	Experimental	16,191.25	3,815.57	1,907.79
Conventional	Experimental	17,988.5	4,599.73	3,252.50

granule loss approximately 30% greater than that of the control group, notwithstanding one instance in which a control specimen recorded a higher loss. This trend continued in test series 2, where the experimental group demonstrated a nearly 40% increase in mean granule loss relative to the control group, underscoring the amplifying effect of natural weathering on asphalt shingles' performance to sub-severe hail. Average granule loss in test series 3 (50.8 mm hailstones) was 7,687.2 mm^2 for the experimental group, differing from the control group, which averaged 2,287.2 mm^2 in granule loss. A striking 108% difference highlights the crucial impact of natural weathering on asphalt shingles. Table 5 shows statistics on both groups, and the results indicate that natural weathering significantly increases granule loss in asphalt shingles following sub-severe exposure. Both impact-resistant and conventional shingles exhibit substantially higher granule loss in the experimental group compared to the control group, with conventional shingles showing slightly greater losses overall. The standard deviations and errors indicate some variability among the test specimens, particularly for conventional shingles, suggesting that individual shingles may respond differently to natural weathering and sub-severe impacts. These results underscore the pronounced effect of environmental exposure on asphalt shingle durability.

Within the control group, the subset of shingles classified as impact-resistant exhibited a mean granule loss of 8,930.5 mm^2 (SD = 3,309.86 mm^2), while the remaining conventional shingles had a similar mean loss of 9,502.0 mm^2 (SD = 3,915.96 mm^2). This suggests that both impact-resistant and conventional shingles experienced comparable levels of granule loss when subjected to two rounds of sub-severe impacts followed by 50.8 mm (2 in.) hail impacts. After two total years of natural weathering and two rounds of sub-severe hail impacts, asphalt shingles exhibited a substantial increase in granule loss. Impact-resistant shingles showed slightly lower mean granule loss, averaging 16,191.25 mm^2 (SD = 3,815.57 mm^2) across the four impact-resistant products compared to 17,988.5 mm^2 (SD = 4,599.73 mm^2) for the two conventional products. These results suggest that impact-resistant designs may offer some degree of mitigation against hail-induced granule loss; however, additional testing with a larger sample set is necessary to validate this trend. The greater granule loss observed in the experimental (naturally weathered) group relative to the control group highlights the role of environmental exposure in degrading asphalt shingles and increasing their susceptibility to hail damage over time.

A Mann-Whitney U test was conducted to compare granule loss between the experimental and control groups. Given the small sample size and the distribution characteristics of the data, the Mann-Whitney U test was selected as a more suitable alternative to the t-test, which assumes normal distribution (Sussex, 2011). This choice was supported by the Kolmogorov-Smirnov (K-S) test, indicating the data did not follow a normal distribution. A statistically significant difference in granule loss was observed between the experimental and control groups ($U = 2.00$, $p = 0.0087$),

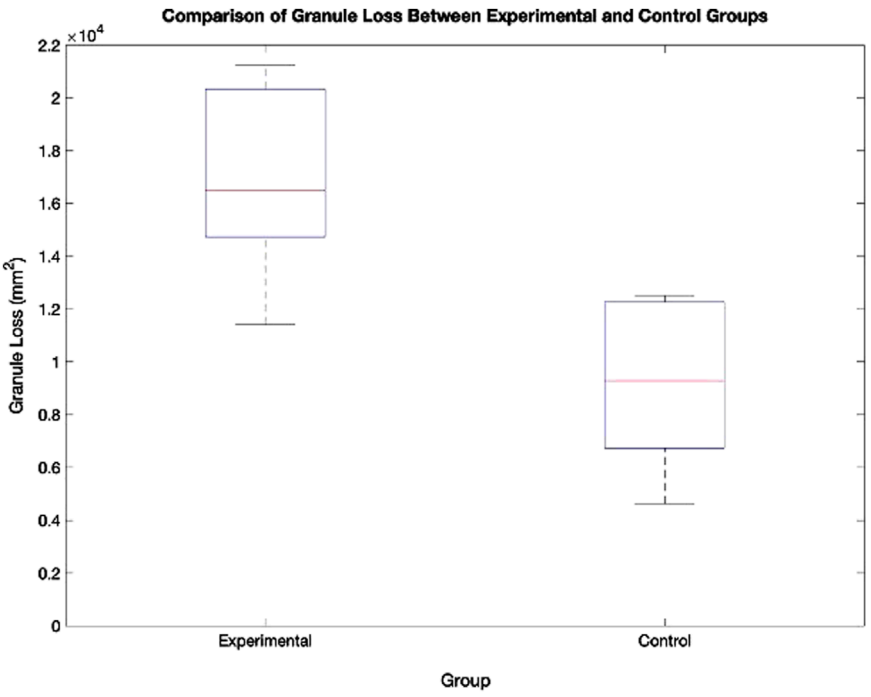

FIGURE 6
Granule loss distribution within the experimental and control groups using the cumulated granule loss after each test series of sub-severe and large hail impacts for each product. Median granule loss for the experimental group was 16,503 mm^2, while the control group was 9,287.5 mm^2.

TABLE 6 Average damage comparison of a single hailstone per test series for granule loss. Baseline test specimens were not impacted with sub-severe hail, reflected by "N/A" in test series 1 and 2—source: Small Hail, Big Problems, New Approach (ZestyAI, 2023). Minor wording and unit clarifications, as well as a column header, were added for clarity. Credit given to Charles Lau with Zesty AI.

Test description	Baseline group (new test specimens)	Control group (conditioned specimens)	Experimental group (naturally weathered specimens)
Test series 1: Small Hail, 17.8 and 25.4 mm (0.7- and 1-inch) Average granule loss per impact after 1 year (500 impacts)	N/A	9.5 mm^2	10.2 mm^2
Test series 2: Small Hail,17.8 and 25.4 mm (0.7- and 1-inch) Average granule loss per impact after 1 year (500 impacts)	N/A	5.7 mm^2	8.0 mm^2
Test series 3: Large Hail, 50.8 mm (2-inch) Average granule loss per impact (20–40 impacts)	20.0 mm^2	57.2 mm^2	192.2 mm^2
Damage Multiplier	1X	2.9X	9.6X

Takeaway: Test series 3 large hail impacts deal 2.9X more damage when preceded by small hail. Large hail can deal 9.6X more damage after both natural weathering and small hail exposure.

indicating a meaningful effect at the 95% confidence level. These results suggest that the conditions applied to the experimental group had a significant effect on granule loss. Visualization of this result is shown in Figure 6, where the experimental group exhibited significantly higher granule loss relative to the control group. The median granule loss in the experimental group was 16,503 mm^2, compared to 9,287.5 mm^2 in the control group, indicating a notable increase in material degradation. The interquartile range (IQR) for the experimental group was 5,601 mm^2, slightly greater than the 5,538 mm^2 observed in the control group, reflecting increased variability with the experimental conditions (Figure 6). These findings suggest that cumulative exposure to natural weathering

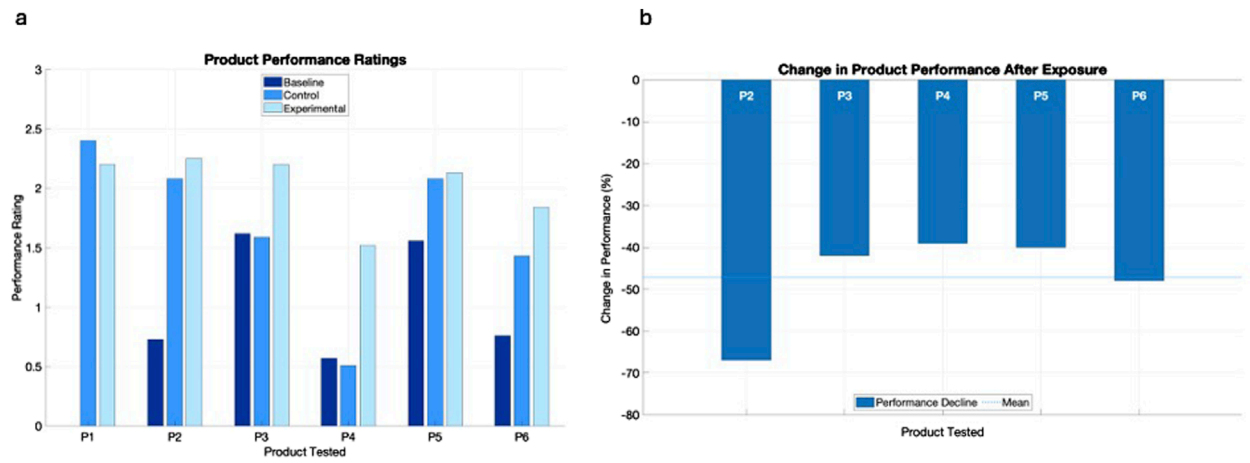

FIGURE 7
Performance decline for overall product ratings. Comparing baseline test specimens (brand new, non-weathered products) impacted with 20–40 hailstones at 50.8 mm (2 in.) in diameter, with the same products naturally weathered (experimental group) for a total of 2 years and impacted with 1,000 ice spheres **(a)**. The average performance decline was 47% while other products ranged from 39% to 67% change **(b)**. **(a)** Overall product performance ratings of brand new products compared to those with sub-severe exposure, including test specimens with and without natural weathering. P1 baseline was not tested. **(b)** Performance declines due to sub-severe ice sphere exposure.

TABLE 7 Average severity scores on a 0–3 scale for baseline (non-weathered and large hail impacts) compared to the experimental group (naturally weathered, sub-severe, and large hail impacts). Scores are normalized on a 0–1 scale to compute the change in performance for each product. Results from this table are plotted in Figure 7b. Product (P1) baseline was not tested and is no longer available for purchase; this is represented in the table as "N/A".

Product	0–3 average severity score		Normalized score (0–1)		Performance change
	Baseline	Experimental	Baseline	Experimental	
P1	N/A	2.20	N/A	0.27	N/A
P2	0.73	2.25	0.76	0.25	−67%
P3	1.62	2.20	0.46	0.24	−42%
P4	0.57	1.52	0.81	0.49	−39%
P5	1.56	2.13	0.48	0.29	−40%
P6	0.76	1.84	0.75	0.39	−48%

in conjunction with sub-severe impacts significantly exacerbates granule loss when compared to test specimens placed in controlled indoor conditions.

Lastly, the average granule loss from a single impact across each test series is displayed in Table 6, highlighting the damage comparison across baseline, control, and experimental groups. Baseline test specimens were brand-new products obtained via the typical roofing supply chain process. These products were not subjected to any natural weathering or sub-severe impacts. Based on the average granule loss per single hailstone impact, as shown in Table 6, hailstones measuring 25.4 mm (1 in.) and below can cause nearly 30% of the granule loss of a 50.8 mm (2 in.) hailstone. The results show that asphalt shingles can be ten times more susceptible to damage after exposure to natural weathering and sub-severe impacts, when compared to new asphalt shingles (Table 6).

3.2 Overall product performance

Performance ratings show specimens exposed to a relatively short period of natural weathering, sub-severe impacts, and large hail (experimental group) had a significant decline compared to the baseline specimens. A poorer performance rating could be expected due to natural weathering, but a combination of natural weathering with sub-severe exposure considerably aids in the reduction in performance (Figure 7). Although the control group was not included in Figure 7b, it was necessary to show the product performance rating in Figure 7a to provide critical insight into the impact natural weathering has on asphalt shingles. The change in performance between the baseline and experimental group is shown in Figure 7b. The average severity scores for both groups were normalized to a 0–1 range (worst to best), and a percent change was calculated (Table 7). Brand new

10.3389/fmats.2025.1603074

TABLE 8 Performance evaluation ratings for experimental and control groups were conducted after each product had completed all test series. The experimental specimens (naturally weathered) performed far worse than the test specimens kept in a conditioned space (controlled group). Abbreviations DN, GL, and BH represent dents, granule loss, and breach (Insurance Institute for Business and Home Safety, 2019).

(a) Performance scores for the experimental group (naturally weathered)						
	P1	P2	P3	P4	P5	P6
Avg. DN Severity Score	2.75	2.81	2.94	2.36	2.44	2.08
Avg. GL Severity Score	3.00	2.98	2.93	2.05	2.83	3.00
Avg. BH Severity Score	0.84	0.95	0.72	0.14	1.12	0.43
Avg. Severity Score	2.20	2.25	2.20	1.52	2.13	1.84
Performance	Poor	Poor	Poor	Marginal	Poor	Poor

(b) Performance scores for the controlled group (conditioned)						
	P1	P2	P3	P4	P5	P6
Avg. DN Severity Score	2.19	2.44	2.83	0.38	2.91	2.23
Avg. GL Severity Score	2.89	2.72	2.59	0.38	2.88	2.77
Avg. BH Severity Score	2.11	1.09	0.94	1.27	2.52	0.73
Avg. Severity Score	2.40	2.08	1.59	0.51	2.08	1.43
Performance	Poor	Poor	Marginal	Good	Poor	Marginal

products outperform older products, even those only 2 years old. When compared to new, non-weathered asphalt shingles, test specimens that experienced both natural weathering and sub-severe impacts within the first few years showed an evident decline in performance, with an average degradation of 47% and reaching as high as 67%.

Overall performance of each product tested was determined following completion of all hailstone impacts, by assessing the severity of breaches, deformations, and granule loss at each 50.8-mm (2-inch) hail impact location, as described in the IBHS Impact Resistance Test Protocol for Asphalt Shingles (Insurance Institute for Business and Home Safety, 2019). The severity of each damage mode was calculated based on the volume of deformation, the amount of granule loss, and the length and depth of the breach. Performance evaluation results of each test specimen in both groups are shown in Table 8. As expected, the experimental group (naturally weathered) test specimens had a worse overall rating than the control group test specimens. The least performance difference was observed in product 5 (P5), a conventional architectural asphalt shingle. Product 1 (P1), a conventional 3-tab asphalt shingle, exhibited 28% less damage following natural weathering compared to its counterpart in the control group, despite both ranking in the poor category based on their average severity scores exceeding 1.8 (Table 8). The reasoning was based on the breach (BH) severity score, indicating that the breaches were more severe on the control specimens. Products 5 (P5) and 6 (P6) also showed worse average severity scores for granule loss (GL) and dent (DN), respectively. These variations in performance across the control and experimental groups are correlated with the variability in the products themselves. However, the other four (one conventional and three impact-resistant) products showed a 20%–55% overall performance decline in the experimental group. A marginal performance indicates the product, when tested, has less reliability to withstand severe weather (specifically hail in this study). Poor performance indicates even less reliability compared to marginal. Products with higher reliability will have a performance rating of good or excellent. No excellent performance rating was observed in this study; however, product 4 (P4) of the control group received a good rating, indicating that the asphalt shingle product exhibited some reliability against severe weather at the time of testing.

Findings from this study indicate that sub-severe exposure presents a significant risk of granule loss on asphalt shingles, with older, naturally weathered roofs exhibiting a higher vulnerability to hail damage. The granule loss can accelerate performance decline (Figure 7b), increasing shingles' vulnerability to future hail damage and ultimately reducing the roof's lifespan. Granule loss was not limited to the typical conventional shingles; rather, it was seen across the spectrum of all asphalt shingle products.

4 Discussion

Current field programs, such as the IBHS Hail Field Study, have aided in the data collection of hail concentrations. One IBHS case study in particular captured approximately 10,000 hailstone impacts within 20 min over a 1-square-foot area (0.09 m^2),

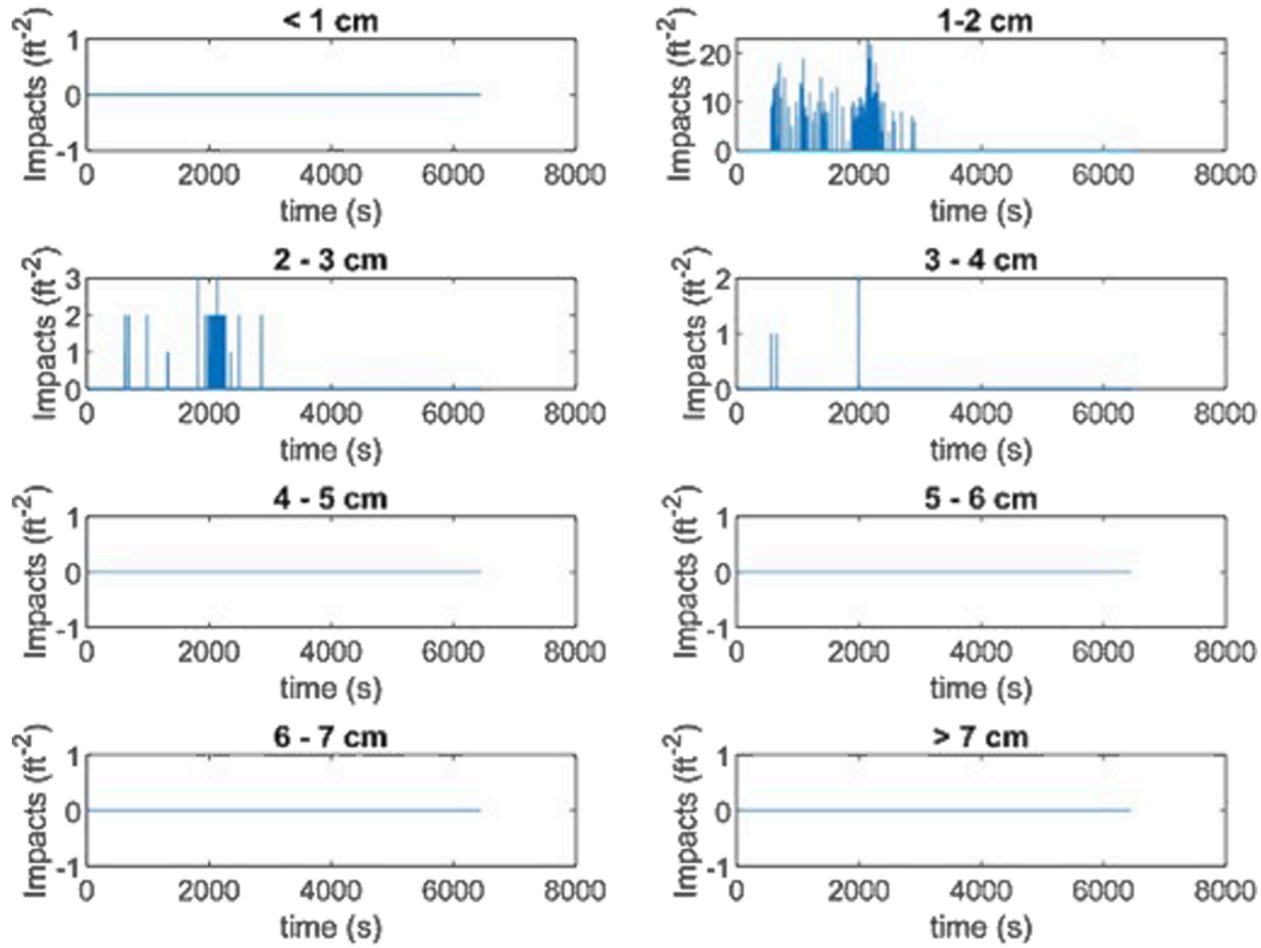

FIGURE 8
A single hail impact disdrometer collected approximately 10,000 impacts per square foot (0.09 m^2) within 20 min. This case is one of many capturing high concentrations of small hail. A few larger hailstones were observed in the large mix of sub-severe hail, most of which are between 1 and 2 cm (0.39 and 0.79 in.). The case study took place on 4 May 2022, in Crowell, T.exas.

highlighting the potential severity of high concentration sub-severe hail events (Figure 8). This case illustrates the wide variability in hailstone concentrations that can occur during storms, often far exceeding the individual impacts used in standardized testing. While limited field data are available, existing observations suggest real-world hail events frequently involve much higher hailstone concentrations than previously recognized. These data, along with the research conducted in this study, support the need for continuing field research in this subject, as sub-severe hailstone areas are poorly represented (Elmore et al., 2022).

In this study, a concentration of 44 sub-severe impacts per square foot (0.09 m^2) was used, based on field-collected data, to simulate a realistic but controlled high concentration hail scenario. Although this value was significantly lower than the most extreme concentrations observed in the field, it was sufficient to demonstrate measurable granule loss and performance degradation in asphalt shingles. These results emphasize that sub-severe hail—historically excluded from many risk models and standardized impact tests—can contribute meaningfully to asphalt shingle deterioration. This underscores the importance of incorporating more realistic hail sizes and concentrations in laboratory testing to reflect field conditions better.

The age of asphalt shingles has proven to be a significant factor in understanding product performance when subjected to hail impacts—yet it remains unaccounted for in current standardized testing protocols. Real-world exposure to environmental stressors, such as daily fluctuations of temperature, wind, precipitation, and ultraviolet radiation, leads to material degradation over time, diminishing a shingles' ability to resist damage. Despite this, most impact testing of asphalt shingles and other roofing materials (such as metal and tile) is conducted on brand-new products. Similarly, sub-severe hail is excluded from these standardized tests, which tend to focus on isolated impacts from large hailstones rather than the more frequent, smaller hail events that occur in the real world. To improve the relevance and predictive accuracy of performance assessments, test standards should evolve to include both product aging and sub-severe hail exposure. These adjustments would allow testing to more accurately reflect the cumulative and progressive nature of damage that roofing materials experience in service.

4.1 Conclusion

This study highlights the damage potential of high concentrations of sub-severe hail, which can significantly reduce a roof's lifespan and accelerate the natural aging process of asphalt shingles. Granule loss is a critical damage mode; it exposes the underlying asphalt to UV radiation, increasing brittleness and accelerating degradation. This form of cumulative damage is not currently addressed in standardized testing protocols or performance assessments, representing a key blind spot in how hail-related roofing risks are understood and evaluated. Our findings show that asphalt shingles exposed to both natural weathering and sub-severe impacts were approximately ten times more susceptible to future damage from subsequent severe hail events. This increased vulnerability underscores the need to account for sub-severe hail in risk assessments and durability standards, as it can meaningfully reduce the overall lifespan of the roof and long-term reliability of asphalt roofing systems.

Following the testing presented in this study, additional testing is planned, following the same methodology and testing across nine additional commonly used asphalt shingle products. While additional testing will require two more years to allow for natural weathering, the current study offers a valuable and novel dataset that addresses a critical gap in understanding of asphalt shingle performance under sub-severe hail exposure, informing ongoing research and risk modelling efforts.

Data availability statement

The raw data supporting the conclusions of this article will be made available by the authors, without undue reservation.

Author contributions

BM: Data curation, Formal Analysis, Investigation, Project administration, Validation, Visualization, Writing – original draft, Writing – review and editing. IG: Conceptualization, Methodology, Resources, Writing – review and editing. FH: Writing – review and editing, Formal Analysis, Software.

Funding

The author(s) declare that no financial support was received for the research and/or publication of this article.

Acknowledgments

The authors gratefully acknowledge Dr. Tanya Brown-Giammanco for developing the foundational idea that guided the direction of this research and for her subject matter expertise during the early stages of the project.

Conflict of interest

The authors declare that the research was conducted in the absence of any commercial or financial relationships that could be construed as a potential conflict of interest.

Generative AI statement

The author(s) declare that no Generative AI was used in the creation of this manuscript.

Any alternative text (alt text) provided alongside figures in this article has been generated by Frontiers with the support of artificial intelligence and reasonable efforts have been made to ensure accuracy, including review by the authors wherever possible. If you identify any issues, please contact us.

Publisher's note

All claims expressed in this article are solely those of the authors and do not necessarily represent those of their affiliated organizations, or those of the publisher, the editors and the reviewers. Any product that may be evaluated in this article, or claim that may be made by its manufacturer, is not guaranteed or endorsed by the publisher.

References

American Society for Testing and Materials (2020). *ASTM D3161/D3161M-20: Standard test method for wind resistance of steep slope roofing products (Fan-Induced method)*. West Conshohocken, PA: ASTM International. Available online at: https://store.astm.org/d3161_d3161m-20.html.

Brown, T. M., Pogorzelski, W. H., and Giammanco, I. M. (2015). Evaluating hail damage using property insurance claims data. *Weather, Clim. Soc.* 7 (3), 197–210. doi:10.1175/wcas-d-15-0011.1

Brown-Giammanco, T. M., Giammanco, I. M., and Estes, H. E. (2021). New asphalt shingle hail impact performance test protocol and damage assessment. *Nat. Hazards Rev.* 22 (4), 04021050. Available online at: doi:10.1061/%28ASCE%29NH.1527-6996.0000509

CAPE Analytics (2025). A rising storm: severe convective storms and the impact of growing hail claims. Available online at: https://capeanalytics.com/resources/growing-hail-claims/(Accessed March 30, 2025).

Elmore, K. L., Allen, J. T., and Gerard, A. E. (2022). Sub-severe and severe hail. *Weather Forecast.* 37 (8), 1357–1369. doi:10.1175/waf-d-21-0156.1

Evan, S. (2024). "Insured catastrophe losses likely to exceed 2023," in *Already above $102bn: aon*. Available online at: https://www.artemis.bm/news/2024-insured-catastrophe-losses-likely-to-exceed-2023-already-above-102bn-aon/(Accessed October 28, 2024).

Freedonia Group (2024). *Residential roofing*. Available online at: https://kc.freedoniagroup.com/reportaction/FF60089_2024/Toc?searchTerms=residential%20roofing (Accessed march 30, 2025).

Heymsfield, A. J., Giammanco, I. M., and Wright, R. (2014). Terminal velocities and kinetic energies of natural hailstones. *Geophys. Res. Lett.* 41 (23), 8666–8672. doi:10.1002/2014gl062324

Heymsfield, A. J., Waite, P. H., Rogers, D. C., Jonsson, H. H., Lance, S., Schmitt, C., et al. (2018). Relationships between the mass and terminal velocity of ice hydrometeors

and their microphysical properties. *J. Atmos. Sci.* 75 (11), 3861–3885. doi:10.1175/JAS-D-18-0035.1

Insurance Institute for Business and Home Safety (IBHS) (2019). IBHS impact resistance test protocol for asphalt shingles. Available online at: https://ibhs.org/wp-content/uploads/2019/06/ibhs-impact-resistance-test-protocol-for-asphalt-shingles.pdf.

Marshall, T. P. (1999). "Protocol for assessment of hail-damaged roofing," in Proceedings of the North America Conference on Roofing Technology, Toronto, Canada, 41–46. Available online at: https://www.researchgate.net/publication/327022554_Protocol_for_Assessment_of_Hail-Damaged_Roofing.

Smith, D. L. (2013). Asphalt composition shingle damage-hail or manufacturing defect? *Interface* 31 (2), 21–28. Available online at: https://iibec.org/wp-content/uploads/2013-02-smith.pdf.

Sussex (2011). *Hole, graham. 2011. mann-whitney handout, version 1.0*. Brighton: University of Sussex. Available online at: http://users.sussex.ac.uk/~grahamh/RM1web/MannWhitneyHandout%202011.pdf.

Swiss Re Institute (2024). *New record of 142 natural catastrophes accumulates to USD 108 billion insured losses in 2023, finds Swiss re institute*. Zurich: Swiss Re. Available online at: https://www.swissre.com/press-release/New-record-of-142-natural-catastrophes-accumulates-to-USD-108-billion-insured-losses-in-2023-finds-Swiss-Re-Institute/a2512914-6d3a-492e-a190-aac37feca15b.

ZestyAI (2023). *Small hail, big problems: a new approach to hail damage assessment*. San Francisco: ZestyAI. Available online at: https://uploads-ssl.webflow.com/5cece3928cdd0a282e3677db/643efa1447664ba4b1df7848_IBHS-ZestyAI-SmallHail-BigProblems-NewApproach.pdf.